Segmented Magnetic Thrust Bearings: Analytic Models and Predictions of Significant Improvement in Dynamic Performance

Zackary W. Whitlow[a], Roger L. Fittro[a], Carl R. Knospe[a]

[a] University of Virgina, Department of Mechanical and Aerospace Engineering, 122 Engineer's Way Charlottesville, VA 22904, USA, fittro@virginia.edu

***Abstract*—Non-laminated magnetic thrust bearings typically exhibit reduced dynamic performance due to eddy currents compared to laminated bearings. Segmented stators have been introduced to increase actuator performance by disrupting eddy current paths in the same manner as laminations in radial magnetic bearings. However, due to manufacturing limitations thrust bearing stators cannot be easily segmented to the extent that they would be considered fully laminated. Therefore, eddy currents continue to affect the dynamic performance significantly. Since analytic models of segmented stators do not presently exist the bearing design process requires the use of finite element analysis (FEA) and experimentation. Here we show, using finite element analysis, that a small number of cuts dramatically improves bandwidth of non-laminated magnetic actuators, validating the segmented design strategy. In addition, existing analytic models of non-laminated magnetic bearings are adapted to a segmented geometry and validated via FEA. Close agreement shows that the analytic model, rather than time consuming FEA, may be used in the design process.**

I. Introduction

Dynamic load capabilities for thrust bearings are critical in many magnetic bearing applications such as machine tool spindles and compressors. High speed milling machine tools may encounter high frequency vibrations due to the cutting process; it is critical that spindle actuators have adequate dynamic capabilities to dampen the response. Thrust bearing dynamic capability is also crucial to compressor performance. Non-laminated thrust bearings leave compressors susceptible to instability during surge and trip events. However, due to manufacturing and material constraints thrust bearings are typically non-laminated, which leads to reduced dynamic capabilities compared to their laminated radial bearing counterparts. Low bandwidth and poor dynamic response of non-laminated thrust bearings often makes them a performance limiting component in both of these applications. Increased dynamic capabilities of thrust bearings would enable a more robust closed loop system, with improved performance [1].

Powder metals, or soft magnetic composites, are one option for reducing eddy current effects. However, powder metalurgy introduces another set of deficiencies. Poor mechanical strength of powder metals precludes its use in thrust disks. Reduced permeability and low saturation flux density compared to the base material should also be considered. Powder metals may be a good option for some applications but will not be considered further here. Instead the focus will be on segmented stator geometry and a corresponding analytic model.

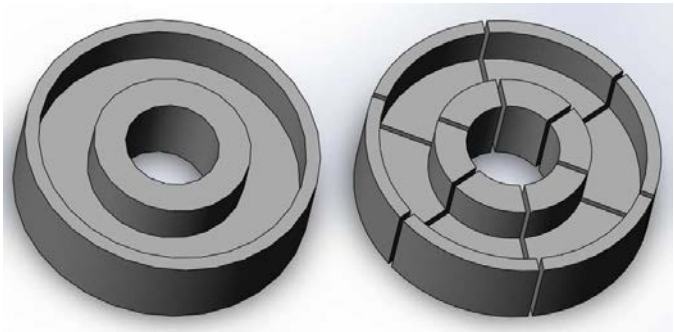

Figure 1: Depiction of a traditional thrust stator and a segmented stator (right).

Segmented axial stators, Fig. 1 right, are a promising method to mitigate problems associated with eddy currents in non-laminated bearings. Stator segmentation serves the same purpose as laminations and could be considered a coarse lamination strategy. By impeding the eddy current loop around the stator periphery with a single cut, or further breaking up the eddy current paths by introducing more stator segments, the geometry approaches that of a laminated thrust bearing. However, the size of these segments is constrained such that eddy current effects cannot be entirely ignored in segmented

Table I: Thrust bearing parameters

Parameter	Definition	Value
r_0	inner radius of inner pole	$51.7\,\mathrm{mm}$
r_1	outer radius of inner pole	$68.3\,\mathrm{mm}$
r_2	inner radius of outer pole	$90.9\,\mathrm{mm}$
r_3	outer radius of outer pole	$101.3\,\mathrm{mm}$
d_1	back iron thickness	$16.5\,\mathrm{mm}$
d_2	pole height	$26.3\,\mathrm{mm}$
d_3	floater thickness	$15.2\,\mathrm{mm}$
g	nominal air gap	$0.5\,\mathrm{mm}$
σ	conductivity	$2\,\mathrm{MS/m}$
μ_r	relative permeability	1000
N	coil turns	166

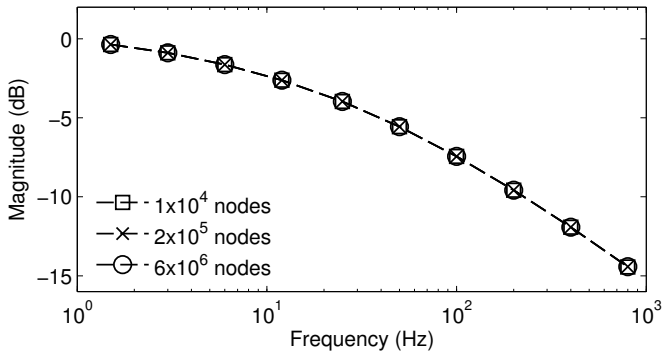

(a) Magnitude: 2-D mesh analysis

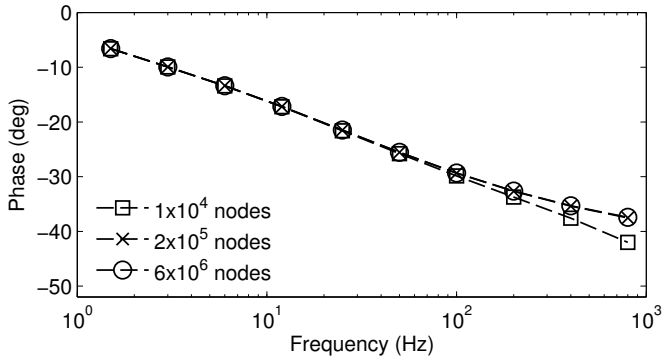

(b) Phase: 2-D mesh analysis

Figure 2: Two dimensional finite element modeling shows magnitude and phase response of the flux density for three mesh resolutions.

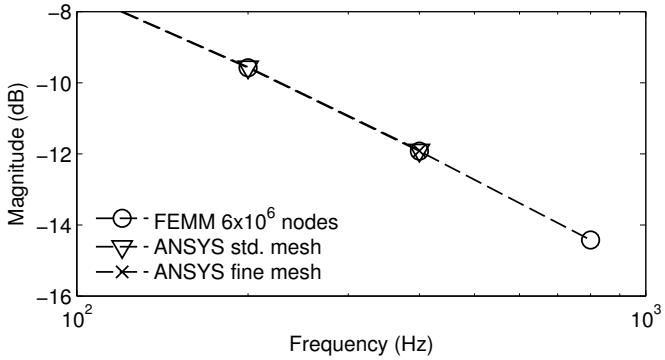

(a) Magnitude: 3-D mesh analysis

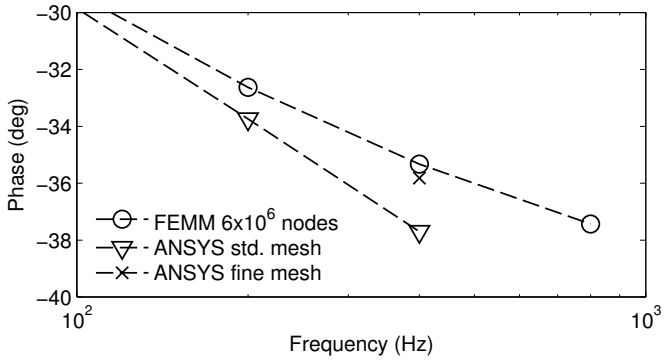

(b) Phase: 3-D mesh analysis

Figure 3: Finite element modeling with perturbation current input and flux output shows magnitude and phase with increasing mesh resolution using FEMM (a) and ANSYS compared to FEMM (b).

thrust bearing models as they can be for fully laminated radial bearings. The thrust disk, or floater, will remain solid to maintain its structural integrity. While segmented designs are currently in use, the authors are not aware of any systematic study of the effect on dynamic performance or of an analytical model for this type of geometry. Without an analytical model it is difficult to determine whether segmentation will yield adequate improvements for a given application.

Analytic models for non-laminated magnetic actuators have been developed by several groups. Feeley developed a two-dimensional (2-D) model for C-type magnetic actuators [2] and Kucera et al. developed a 2-D model for non-laminated axisymmetric geometries [3]. Both of these models account for the impedance of flux due to eddy currents but fail to account for reduced air gap flux. These models were further advanced by Zhu et al. who included the reduced air gap flux due to eddy currents to develop 2-D models for axisymmetric [4] and C-type [5] magnetic actuators. Zhu demonstrated with these 2-D analytical models that it is possible to accurately predict performance of C-type and solid axisymmetric non-laminated magnetic actuators. However, segmented stator geometries were not considered. The purpose of this work is to extend Zhu's concepts to segmented thrust bearings and develop a simple analytic model. Preliminary validation of the model for a test case of an existing thrust bearing geometry shows close agreement between analytic and finite element analysis.

II. Theory

Zhu et al. developed two models for non-laminated magnetic actuators [4], [5], one for an axisymmetric geometry and another for a C-type geometry. For each of these models, the geometry is divided into regions based on flux path and an effective reluctance is calculated for each region. In the axisymmetric case, the 2-D geometry is divided into six regions [4]. Regions 1 and 3 include parts of the floater (i.e. thrust disk), the air gaps, and the portion of the stator that borders the air gaps. Region 2 is the central portion of the floater. Regions 4, 5, and 6 make up the remaining parts of the stator. For the C-type actuator there are three regions; the floater, the air gaps, and the stator [5]. Using magnetic circuit theory and partial differential equations to model the skin effect produced by eddy currents, Zhu *et al.* developed analytic models of effective reluctance, R_1 ... R_6 for regions of an axisymmetric geometry and R_f, R_g, and R_s for the floater, air gap, and stator regions of a C-type geometry [4], [5]. This is the starting point for our development of an analytic model for segmented thrust bearing geometries.

Zhu's axisymmetric model assumed a geometry without a center hole which is not typical of thrust bearings. To accommodate geometries with a center hole the effective reluctance of Zhu's actuator regions 1 and 6 [4] which border the central axis of the actuator were modified. The derivation

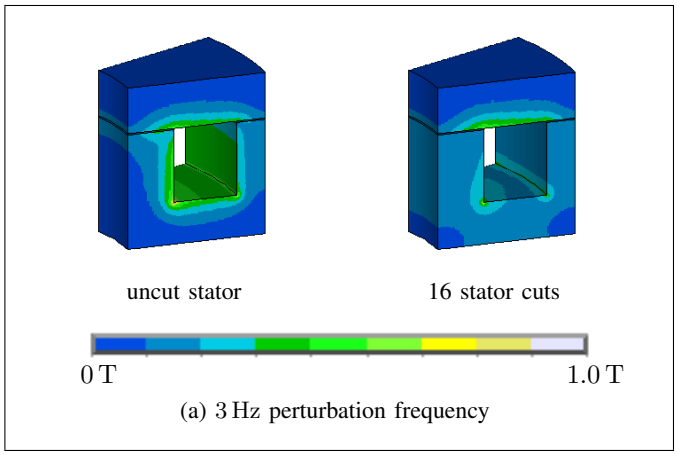

(a) 3 Hz perturbation frequency

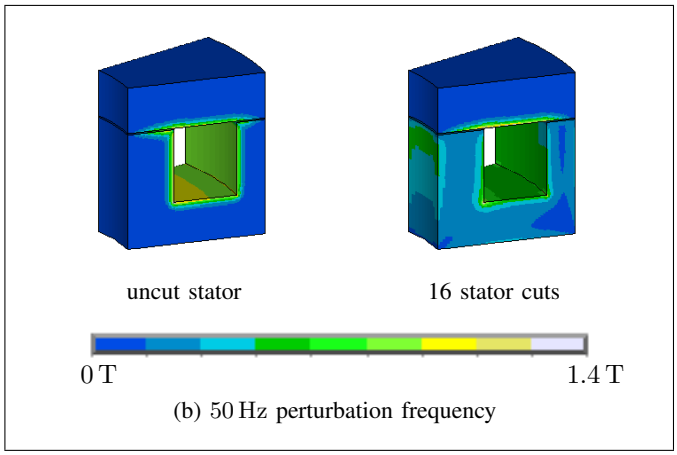

(b) 50 Hz perturbation frequency

Figure 4: Magnetic flux density magnitude for a stator with 0 or 16 cuts. Floater is not cut.

results (details to be published) are as follows

$$R_1(s) = \frac{g\alpha_1}{r_1 2\pi\mu_0} \frac{I_1(\alpha_1 r_0)K_0(\alpha_1 r_1) + I_0(\alpha_1 r_1)K_1(\alpha_1 r_0)}{I_1(\alpha_1 r_1)K_1(\alpha_1 r_0) - I_1(\alpha_1 r_0)K_1(\alpha_1 r_1)} \quad (1)$$

$$R_6(s) = \frac{d_2\alpha}{r_1 2\pi\mu_0\mu_r} \frac{I_0(\alpha r_0)K_1(\alpha r_1) + I_1(\alpha r_1)K_0(\alpha_1 r_0)}{I_1(\alpha r_1)K_1(\alpha r_0) - I_1(\alpha r_0)K_1(\alpha r_1)} \quad (2)$$

$$\alpha_1 = \sqrt{\frac{2\alpha}{\mu_r g}} \qquad \alpha = \sqrt{s\sigma\mu_0\mu_r},$$

where $I_n(\cdot)$ is the nth-order modified Bessel function of the first kind, $K_n(\cdot)$ is the nth-order modified Bessel function of the second kind, σ is the conductivity, r_0 is the inner radius of the inner pole, r_1 is the outer radius of the inner pole, g is the air gap distance, d_2 is the pole height, μ_0 is the magnetic permeability of free space, and μ_r is the relative permeability.

The analytic model was then modified to accommodate a segmented stator. An axisymmetric thrust bearing cut like a pie has segments that resemble individual C-type actuators that are curved and fit together. Therefore, Zhu's C-type model for the segmented geometry was used as a starting point. If the floater and stator were cut Zhu's C-type model could be used directly on each segment and the pieces could be assembled as a parallel magnetic circuit to determine the total

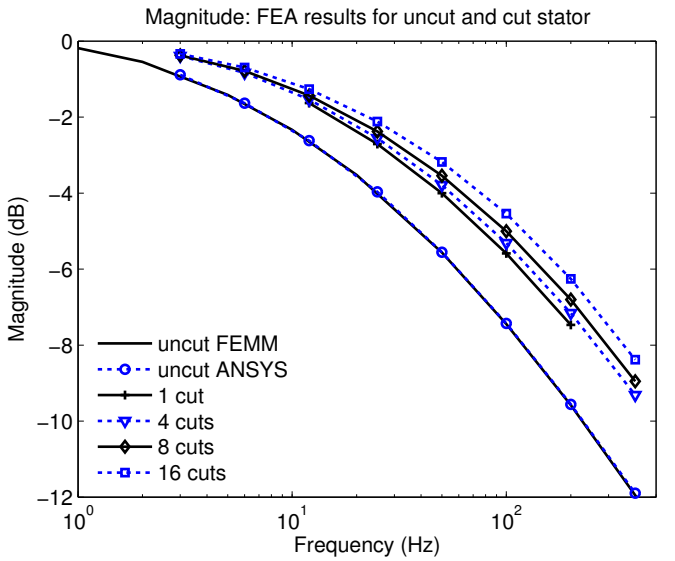

(a)

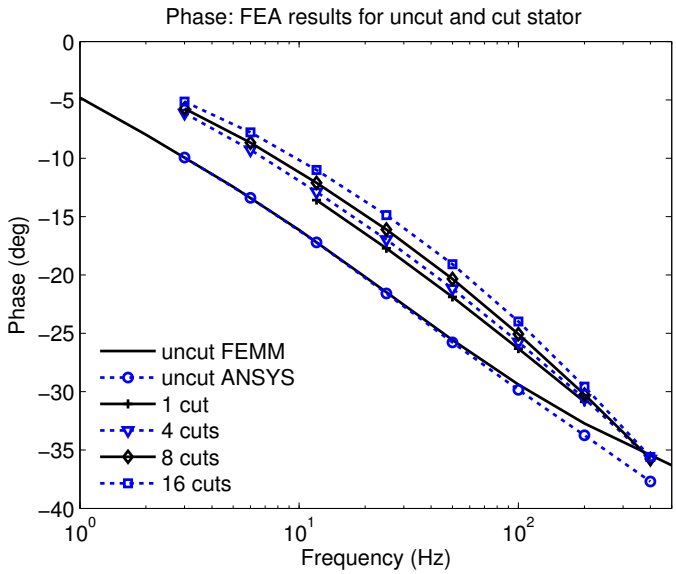

(b)

Figure 5: FEA Magnitude and phase from of thrust bearing with unsegmented stator or cut stator.

reluctance. However, a segmented floater is not practical in rotating machinery due to mechanical strength requirements. Since the C-type model has separate reluctance terms for the floater and stator the floater disk can be modeled as a c-type floater by neglecting the curvature and using the average circumference of the inner and outer poles as the length parameter. This strategy assumes the floater has a single cut since a C-type floater has two unconnected ends. However, if the length of a C-type actuator, pole circumference in this case, is much greater than the pole width then the electromagnetic field interactions at the ends of the actuator contribute little to the dynamics of the entire actuator [6]. Another difference between the C-type geometry and a segmented thrust bearing is the different widths of the inner and outer poles. A simple solution is to use the average length and width of the inner

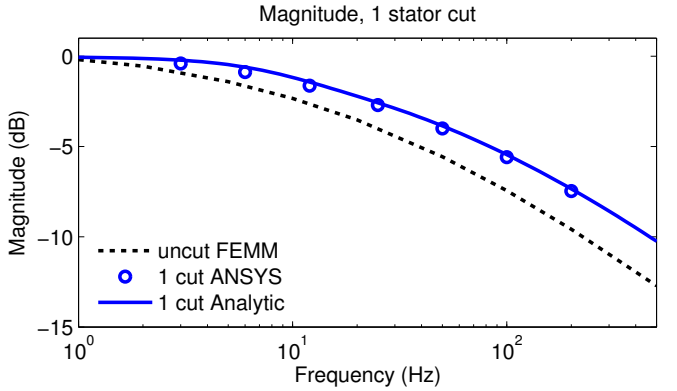

(a)

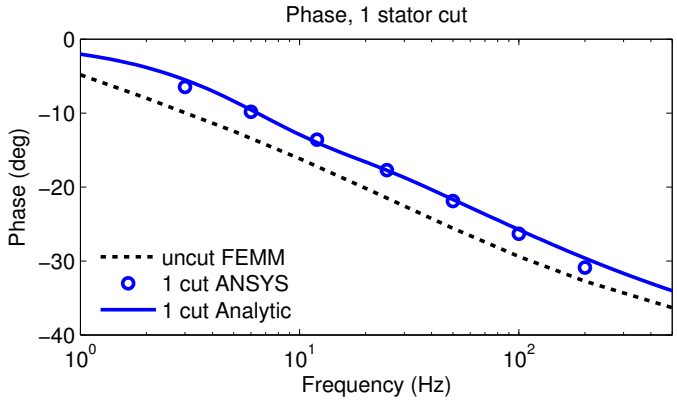

(b)

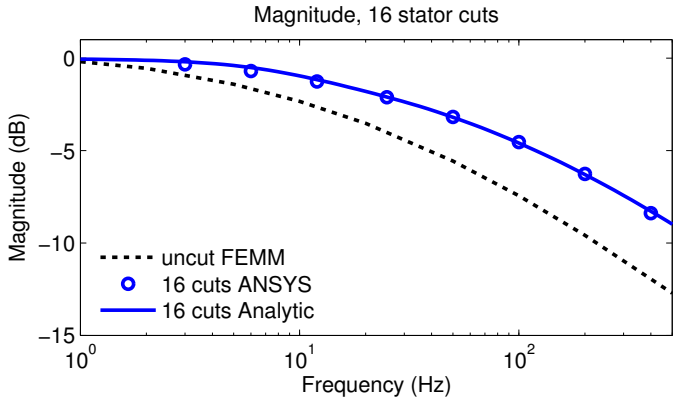

(c)

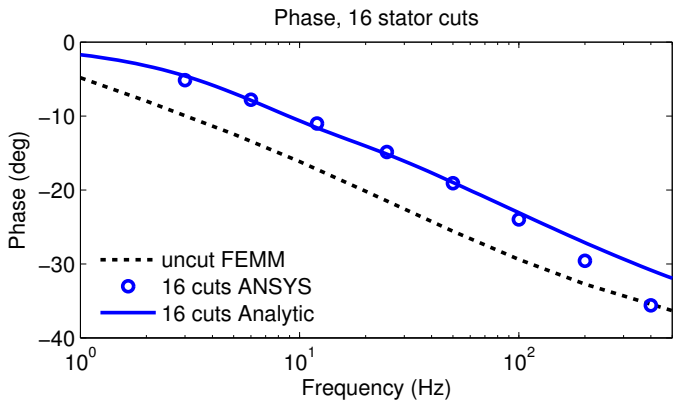

(d)

Figure 6: Magnitude and phase from FEA of thrust bearing with unsegmented stator or cut stator.

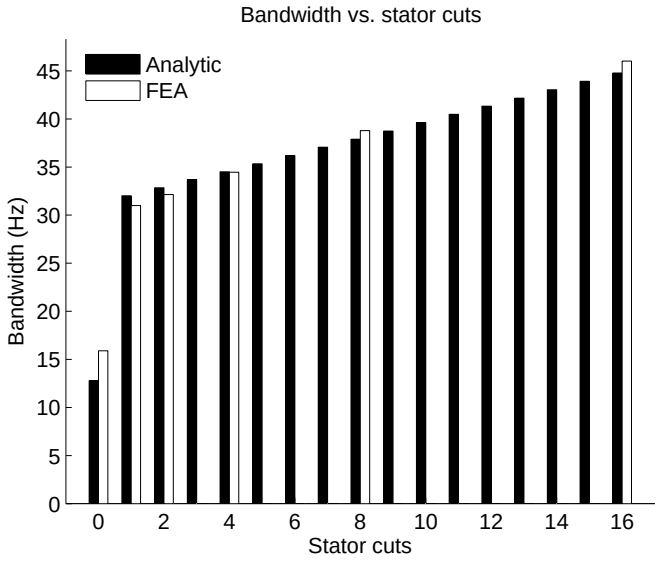

Figure 7: Actuator bandwidth predicted using the analytic model or FEA (0, 1, 2, 4, 8, and 16 stator cuts).

and outer poles which was the approach chosen here. Using Zhu's full analytic model of reluctance for floater, air gap and stator regions where the reluctance is the product of a static term, R^0, and dynamic term, R^d, as follows

$$R_i = R_i^0 R_i^d(s) \tag{3}$$

The total reluctance of an actuator with m stator segments is then

$$R = \frac{R_s^0 R_s^d(s)}{m} + R_f^0 R_f^d(s) + 2R_g^0 R_g^d(s) \tag{4}$$

The transfer function from perturbation current, i_p, to perturbation flux, ϕ_p, then becomes

$$\phi_p(s) = \frac{N}{\frac{R_s^0 R_s^d(s)}{m} + R_f^0 R_f^d(s) + 2R_g^0 R_g^d(s)} i_p(s) \tag{5}$$

The perturbation force F_p is then determined using the Maxwell stress tensor [4], [7].

$$\begin{aligned} f(t) &= \frac{1}{2\mu_0} \oint_S \mathbf{B}^2(t,r)\mathrm{d}S \\ &= \frac{1}{2\mu_0} \oint_S [\mathbf{B_b}^2 + 2\mathbf{B_b}\mathbf{B_p}(t,r) + \mathbf{B_p}^2(t,r)]\mathrm{d}S \end{aligned} \tag{6}$$

Such that for a small perturbation current we have the following relationship.

$$\mathbf{B_p}^2(t,r) \approx 0$$

$$\begin{aligned} F_p(s) &= \frac{1}{\mu_0}\left[\int_{r_0}^{r_1} \mathbf{B_b}\mathbf{B_p}(s,r)\cdot 2\pi r\mathrm{d}r \; + \int_{r_2}^{r_3} \mathbf{B_b}\mathbf{B_p}(s,r)\cdot 2\pi r\mathrm{d}r\right] \\ &= \frac{\phi_b}{\mu_0}\left(\frac{1}{A_1}+\frac{1}{A_2}\right)\phi_p(s) \\ &= \frac{\phi_b}{\mu_0}\left(\frac{1}{A_1}+\frac{1}{A_2}\right)\left[\frac{N}{\frac{R_s^0 R_s^d(s)}{m} + R_f^0 R_f^d(s) + 2R_g^0 R_g^d(s)}\right] i_p(s) \end{aligned} \tag{7}$$

III. Results of Finite Element Analysis

To support the validity and accuracy of the analytic model for segmented thrust bearings developed in section II, a sample test case was chosen to analyze and compare with FEA results. The test case chosen is an existing thrust bearing on the compressor surge test rig developed at the University of Virginia [8], [9]. The geometric and material parameters are summarized in Table I. Finite element analysis was performed using two different codes, Finite Element Method Magnetics (FEMM) [10] and ANSYS Mechanical, over a range of current excitation frequencies. Flux magnitude and phase were plotted to determine the minimal mesh resolutions required, Figs. 2,3.

Flux magnitudes are similar for each of the mesh resolutions tested in FEMM, Fig. 2a. However, for the lowest resolution mesh, the phase diverges from that of the finer meshes for frequencies above $100\,\mathrm{Hz}$, Fig. 2b. At higher frequencies the eddy-current induced skin effect restricts the flux path to the surface region adjacent to the coil, Fig. 4. With the flux concentrated in fewer elements near the surface and a steep flux gradient at the edge of this region a finer mesh resolution is required in order to obtain an accurate result. The highest mesh resolution (6 million nodes) was used for subsequent FEMM-related analyses.

To analyze the effect of stator cuts, 3-D FEA is required. For benchmarking the 3-D ANSYS model the uncut geometry with 64-fold symmetry was used for comparison of mesh resolutions. Stator segmentation disrupts the axisymmetric characteristic of the actuator requiring that larger wedges be modeled. The worst case, from a computational perspective, being a 2-fold symmetry model for a stator with 1 or 2 cuts. Stator cuts are modeled by an air gap or by using a current parallel boundary condition.

3-D FEA showed the same phase inaccuracies at higher frequencies that were observed with 2-D FEA when standard mesh resolution was used, Fig. 3. The flux magnitudes predicted using the 3-D model (ANSYS) matched the 2-D results (FEMM) well. Using a finer 3-D mesh the phase results at $400\,\mathrm{Hz}$ are very close to matching the 2-D results. However, due to excessively large times required for computation, up to $72\,\mathrm{hr}$ for the 64-fold symmetry model, the standard mesh size was used for all subsequent 3-D FEA.

Plots of flux distribution in ANSYS clearly show the effect of stator segmentation on flux distribution, Fig. 4. Actuators with an uncut stator and a stator with 16 cuts were driven at frequencies of $3\,\mathrm{Hz}$ and $50\,\mathrm{Hz}$. The magnitude of the predicted flux distributions were plotted and are shown in Fig. 4. With an uncut stator, eddy currents are more severe which leads to a dramatic skin effect restricting the flux path close to the iron surface. However, with a segmented stator, the eddy current loops circumscribing the stator are broken, restricting eddy currents to smaller regions. Smaller eddy current loops reduce the effective reluctance in the iron which leads to a more uniform flux distribution. The effect this has on dynamic performance is significant.

Flux magnitude and phase were predicted by FEA for perturbation frequencies between 3 and $400\,\mathrm{Hz}$, Fig. 5. With a single stator cut a significant shift in magnitude can be seen. With smaller shifts for additional cuts, Fig. 5a. FEA also predicts a phase improvement with increasing number of stator cuts, Fig. 5b. These results show that non-laminated thrust bearings with a segmented stator can significantly improve dynamic performance. For frequencies above $100\,\mathrm{Hz}$ the phase lag predicted by 3-D FEA is an overestimate. This is obvious when comparing ANSYS and FEMM results shown in Fig. 5b for the uncut geometry. However, by comparing only 3-D FEA results it may be concluded, in spite of the FEA overestimate, that a significant reduction in phase lag will occur Fig. 5b. Focus will now be directed towards an analytic model for non-laminated thrust bearings, which will make the process of designing and modeling segmented or unsegmented thrust bearings much faster by eliminating the reliance on FEA for accurate results.

IV. Results of Analytic Analysis

FEA shows that the effective reluctance in the iron which increases with excitation frequency is reduced by cutting the stator into segments. The analytic model presented here closely matched the results of FEA, Fig. 6. For a stator with 1 cut the analytic model closely matched the normalized flux magnitude predicted by FEA, Fig. 6a, where FEA (FEMM) results from the uncut geometry are also shown as a reference. Fig. 6b shows close agreement for the phase predicted by the analytic model and FEA model for frequencies below $200\,\mathrm{Hz}$. It is likely that the analytic model is more accurate than FEA at frequencies above $100\,\mathrm{Hz}$ since the analytic model does not suffer from the effects of discretization. The analytic results for a stator with 16 cuts also agree well with FEA, Figs. 6c and 6d, but with a similar discrepancy in phase at higher frequencies due to the standard mesh density used for FEA.

Plotting the bandwidth as a function of frequency shows once again that a single cut in the stator has the greatest impact on performance, Fig. 7. The relationship between bandwidth and cuts appears to be affine for 1 through 16 cuts, Fig. 7, with cuts beyond the first resulting in smaller bandwidth improvement. With 8 cuts in the stator, well within manufacturing and material constraints, a 2.5-fold increase in bandwidth is predicted. These results show that a segmented geometry will improve dynamic performance of non-laminated thrust bearing.

V. Conclusions

Existing analytic models for non-laminated C-type and axisymmetric magnetic actuators have been further developed for application to segmented thrust bearings. This analytic model was applied to a test case which predicted significant improvements in dynamic performance with segmentation and closely matches predictions from FEA. Enhanced dynamic performance was predicted with modifications that are well within practical manufacturing constraints, validating the segmentation strategy. Enhanced dynamic performance due to segmentation may not be as significant for all size bearings and geometries. Future studies will address the effect of geometric parameters on performance enhancement achieved via segmentation. Analysis of other geometries will also further assess the validity of the analytic model.

REFERENCES

[1] C. R. Knospe and L. Zhu, "Performance limitations of non-laminated magnetic suspension systems," *IEEE Transactions on Control Systems Technology*, vol. 19, no. 2, pp. 327–336, Mar. 2011. [Online]. Available: http://ieeexplore.ieee.org/lpdocs/epic03/wrapper.htm?arnumber=5463016

[2] J. J. Feeley, "A simple dynamic model for eddy currents in a magnetic actuator," *IEEE TRANSACTIONS ON MAGNETICS*, vol. 32, no. 2, pp. 453–458, March 1996.

[3] L. K. M. Ahrens, "A model for axial magnetic bearings including eddy currents," *Proc. Third Int. Symp. Magnetic Suspension Technology*, vol. 2, pp. 421–438, Dec. 1995.

[4] L. Zhu, C. Knospe, and E. Maslen, "Analytic model for a nonlaminated cylindrical magnetic actuator including eddy currents," *IEEE Transactions on Magnetics*, vol. 41, no. 4, pp. 1248–1258, Apr. 2005. [Online]. Available: http://ieeexplore.ieee.org/lpdocs/epic03/wrapper.htm?arnumber=1420680

[5] L. Zhu and C. Knospe, "Modeling of nonlaminated electromagnetic suspension systems," *IEEE/ASME Transactions on Mechatronics*, vol. 15, no. 1, pp. 59–69, Feb. 2010. [Online]. Available: http://ieeexplore.ieee.org/lpdocs/epic03/wrapper.htm?arnumber=4838650

[6] L. Zhu, "Non-laminated magnetic actuators: Modeling and performance limitations," Ph.D. dissertation, University of Virginia, May 2005.

[7] D. J. Griffiths, *Introduction to Electrodynamics*. Prentice-Hall, 1989.

[8] S. Y. Yoon, "Surge control of active magnetic bearing suspended centrifugal compressors," Ph.D. dissertation, University of Virginia, December 2011.

[9] L. Z. A. P. E. Yoon, Se Young, *Control of Surge in Centrifugal Compressors by Active Magnetic Bearings*. Springer, 2013.

[10] D. C. Meeker. Finite element method magnetics. Version 4.2 (11Apr2012). [Online]. Available: http://www.femm.info/wiki/HomePage